Available online at www.pelagiaresearchlibrary.com

Pelagia Research Library

Advances in Applied Science Research, 2012, 3 (5):3045-3052

ISSN: 0976-8610
CODEN (USA): AASRFC

Synthesis and Characterization of Polyurethane Nanocomposite from Castor Oil- Hexamethylene Diisocyanate (HMDI)

Krushna Chandra Pradhan and P. L. Nayak*

P.L Nayak Research Foundation, Synergy Institute of Technology, Bhubaneswar, Odisha, India

---

ABSTRACT

Polyurethanes (PUs) are one of the most versatile classes of materials today and their demand as a high performance industrial material continues to grow. The wide application of Pus necessitates understanding the chemistry and structural elements that improve the thermal stability and flame retardancy as these are important prerequisites to obtain tailor-made products for high performance applications such as in aggressive environments. . In the present research program, some polyurethane nanocomposites have been prepared from a natural oil like castor oil using HMDI and organically modified clay. Polyurethanes and their nanocomposites have been characterized by using some sophisticated methods like FTIR, SEM, XRD, TGA, and mechanical testing. Hydrophobic nanoparticles and nanocomposite of 1,4-hexamethylene diisocyanate (HMDI)-modified PU nanoparticles (PU-NPs) have been synthesized at ambient temperatures. The platelet-like nanocrystals become pseudospherical after modification with HMDI and the size increases or decreases depending on diisocyanate concentration compared to the ungrafted particles as revealed by scanning electron microscopy (SEM) results. The obtained nanocrystals were characterized by means of the FT-IR and X-ray diffraction (XRD) techniques.

Key Words : Polyurethane; HMDI; Nanocomposite; FTIR , SEM

INTRODUCTION

Polymer- nanocomposites have recently gained a great deal of attention because they offer a great potential to provide superior properties when compared to\pure polymers and conventional filled composites. The properties include high dimensional stability, high heat deflection temperature, reduced gas permeability, improved flame retardance, and enhanced mechanical properties [1–3].

Polyurethanes (PUs) are unique polymer materials with a wide range of physical and chemical properties. With welldesigned combinations of monomeric materials, PUs can be tailored to meet diversified demands of various applications such as coatings, adhesives, fibers, thermoplastic elastomers, and foams. However, PUs also have some disadvantages, such as low thermal stability and low mechanical strength, etc. To overcome these disadvantages, a great deal of effort has been devoted to the development of nanostructured polyurethane (PU)/montmorillonite (MMT composites in recent years/

Segmented polyurethanes, and in particular poly- (urethane urea)s (PUUs), are currently used in a variety of blood-contacting applications in biomedical devices. For example, the Arrow International LionHeart and Abiomed's AbioCor cardiac assist devices utilize PUU elastomers in the blood pump as well as in other locations. In general, biomedical PUUs possess good biocompatibility and flexural fatigue characteristics but, because of the low Tg and relatively high concentration of soft segments, are relatively permeable to air and water vapor. The latter can lead to potential problems, particularly in completely implantable devices.

Castor oil is world's one of the most useful and economically important non-edible, nonvolatile natural vegetable oil. Pt is a unique industrial oil, due the presence of triglycerides of hydroxyl fatty acid known as ricinoleic acid. The

ricinoleic acid content is about 87-90%. Ricinoleic acid is an 18 carbon hydroxylated fatty acid having one double bond at the 9^{th} & 10^{th} carbon. Nayak and coworkers have carried out extensive research work on IPN derived from Castor Oil and a multitude of diisocyantes.

Cloisite 30B is methyl, tallow, bis-2 hydroxyethyl, quaternary ammonium, where tallow is 65% C18, 30% C16, and 5% C14. Clay minerals are widely used materi-als in drug products as delivery agents [12]. Montmoril-lonite (MMT) can provide mucoadhesive capability for the nanoparticle to cross the gastrointestinal (GI) barrier [13]. MMT is also a potent detoxifier, which belongs to the structural family of 2:1 phyllosilicate. MMT could absorb dietary toxins, bacterial toxins associated with gastrointestinal disturbance, hydrogen ions in acidosis and metabolic toxins such as steroidal metabolites asso-ciated with pregnancy [14].

Recently Nayak and coworkers have carried out extensive research work on castor oil -based interpenetrating polymer networks (15-19). This communication presents the result of nano composite polyurethane using castor oil and hexamethylene diisocyanate.The composites were characterized usingn FTIR, SEM, TGA and XRD methods.

MATERIALS AND METHODS

Because the synthesis involved toxic and reactive diisocyanates, all the necessary precautions were taken regarding their safe handling and performing their reactions.

2.1. Synthesis of the polyurethanes

The castor oil was dried in a vacuum, for 10 h at 70^0C in a water bath before being used. The dried castor oil was placed in a three-necked, round-bottom flask equipped with a stirrer, dropping funnel and thermometer. The temperature was maintained at 70^0C and the diisocyanate was added under constant stirring. Then reaction mixtures were cast into preheated mould coated with silicon and heated in an oven at 110^0C for 12 h. The goal of this study was to prepare castor oil based polyurethanes with different types of diisocyanate (toluene diisocyanate, and hexamethylene diisocyanate). Polyurethane formation was confirmed by ATR-FT-IR studies by detecting the urethane band at 1515 cm−1 and the appropriate NCO/OH ratio was determined based on which, polyurethane nanocomposites (PUNCs) were further synthesized with different clay loadings.

2.2 Synthesis of HMDI-based Polyurethane Nanocomposites

HMDI and castor oil were dehydrated under vacuum overnight at room temperature and 60^OC, respectively. The clay was dehydrated in an oven at 100^OC overnight before use. Three sets of samples containing 1, 2.5 and 5 wt. % of OMMT were prepared as follows through in situ polymerization technique: the desired weights of polyol and OMMT were measured in a plastic flask (with nitrogen inlet and temperature control jacket) and mixed with a propeller stirrer at 1200rpm for 2 h at 70◦C. The dispersions of organoclay were then sonicated for 30 min at 60◦C with an external cooling bath. The ultrasonication process was performed at a frequency of 20 kHz with an inlet ultrasound power of around 1W/mL (UIP 1000hd ultrasonic processor, Hielscher ultrasound technology).

1. Instrumentation :

1.1. FT-IR Analysis

A Vector-22 FT-IR spectrometer (Bruller Optics, Billerica, MA) with a resolution of 1 cm-1 from 4000 to 400 cm-1 using KBr pellets was used to verify the completion of the resin curing reaction and the presence of free isocyanate groups (NCO) in cured nanocomposites**IR spectra** The Fourier transform infrared (FT-IR) spectra were recorded on a Nicolet 8700 spectrometer, in the range 400–4,000 cm^{-1}.

1.2. TGA

The thermal degradation pattern of the pristine PU as well as the PU-C30B nanocomposites were determined by Thermogravimetric Analysis (TGA, Universal V4.5A, TA Instruments) under a nitrogen atmosphere. The samples were heated from room temperature to 600 ºC at a rate of 10ºC/min. The weight change of each sample was recorded as a function of temperature and the results were compared to pure clay. Given that the inorganic clay has much greater decomposition temperature than the organic polymer, the content of the clay inside the samples was estimated from the comparison of curves.

3.3 . X-ray diffraction (XRD) analysis :

PowderXRD patterns were obtained using Simens/Bruker D5000 Diffractometer, with monochromatic Cu Ka radiation (k = 0.15418 nm). Scans were obtained in the 2h range = 20–60_, with a step size of 0.02_ every 1 s.

3.4. Mechanical properties

Tensile property was measured according to ASTM D 638 by a universal testing machine (LR 50K, Lloyd Instrument, UK) with a gauge length of 20 mm and a crosshead speed of 5 mm/min.

3.5 . SEM

Morphology of the Poly(FAn)/c-MWCNTS composite was investigated using a Philip XL 30 SEM at an accelerating voltage of 25 kV. The sample was fractured at liquid nitrogen temperature and then was coated with a thin layer of gold before observation

RESULTS AND DISCUSSION

1.3. FTIR Analysis

FTIR spectra of the nanocomposites were recorded in FTIR Nicolet, Impact 410 spectrophotometer. Small quantities of the finely powdered samples were dispersed in pure dried KBr and further ground to a fine mixture in a mortar before pressing to form transparent KBr pellets for analysis. FTIR spectra of PUs (and polyol-based polyurethanes) are well known to be sensitive to hard domain organization and the urea and urethane hydrogen bonding. Consequently, to understand the possible reactions that may occur among the reactants (HMDI, PU and C 30B), the FTIR spectra of C 30B, HMDI cured PU and HMDI cured PU/C 30B nanocomposites containing 2.5 wt% modified clay (SM-15) are recorded . The characteristic absorptions peaks of the PU are observed at 3306 cm-**1** (N–H stretching frequency), 2925–2852 cm-**1** (–CH**2**– and –CH**3** stretching frequencies), 1731 cm-**1** (carbonyl urethane stretching), 1526 cm-**1** (CHN vibration), 1223 cm-**1** (coupled C–N and C–O stretching), and 1079 cm-**1** (C–O stretching). Comparison of neat PU(SM-12) with the nanocomposite, i.e., (SM-15) indicates that all the characteristic absorptions of PU remain unchanged in the PU/C 30B(SM-15) nanocomposite. But the urethane characteristic peaks at 1732 and 1526 cm-**1** are enhanced due to the formation of more number of urethane linkages during the course of the curing reaction. Absence of peak at 2270 cm-**1** (–NCO group) confirms that all the HMDI have been used in the curing reaction. In case of the nanocomposite (SM-15), it is evident that the characteristic absorption peaks at 522 cm-**1** (Al–O–Si deformation) and 1047 cm-**1** (Si–O in plane stretching) are observed. Furthermore, the extra absorptions at 3700–3400 cm-**1** (N–H stretching) and 1240 cm-**1** (amide vibration) indicate the formation amide structure between C30B and the PU matrix. The FTIR spectra also reveals that the nanocomposite with Cloisite 30B(SM-15) has the characteristic peaks at 1731 cm-**1** (carbonyl urethane stretching), 1526 cm-**1** (C–NH– vibration), 1223 cm-**1** (coupled C–N and C–O stretching), 1079 cm-**1** (C–O stretching), 522 cm-**1** (Al–O–Si deformation), and 1047 cm-**1** (Si–O in plane stretching), indicating that the polymer chains have intercalated into the gallery of C30B .Some polymer chain ends with –NCO groups come closer to the vicinity of the clay galleries during nanocomposites preparation and react with CH2CH2OH group of the quaternary ammonium ions to produce urethane linkage, –CO–NH–, leading to a fine dispersion of the clay particles.

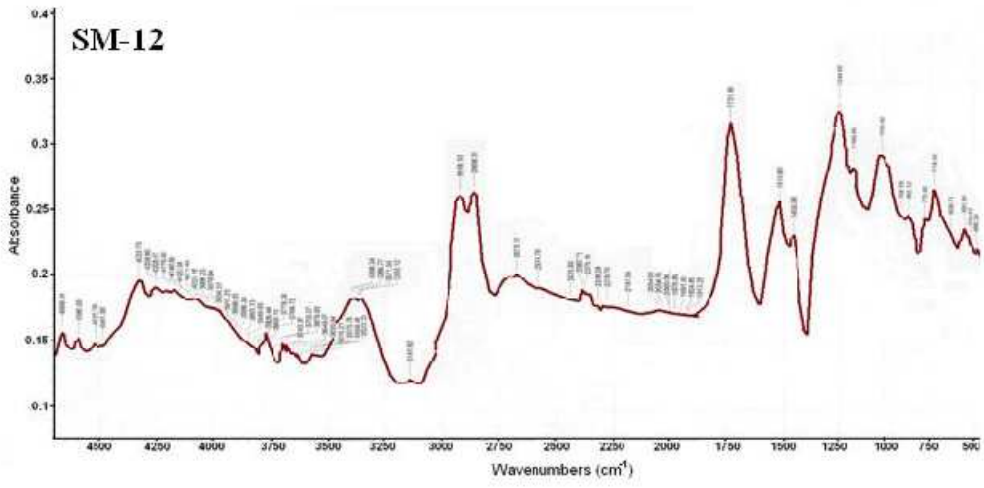

Fig. 1 FTIR of Polyurethane Nanocomposite of HMDI+ C30B - 0 % (SM-12)

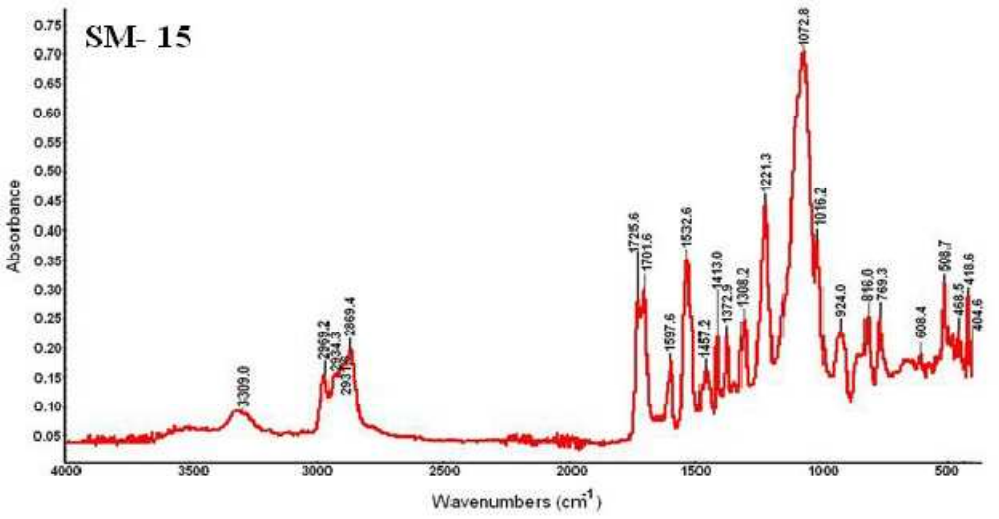

Fig, 2 FTIR of Polyurethane Nanocomposite of HMDI+ C30B-2.5 % (SM-15)

1.4. Thermogravimetric analysis

The thermal degradation of polyurethane occurs in two stages: the first stage is mainly governed by the degradation of the hard segment and the second stage correlates well with the degradation of the soft segment. Generally, clay particles can enhance the thermal stability of polymer by acting as thermal insulator and mass transport barrier to the volatile products generated during decomposition. The effect of clay as thermal insulator and mass transport barrier on thermal stability can be increased with improving the dispersibility of organoclay.

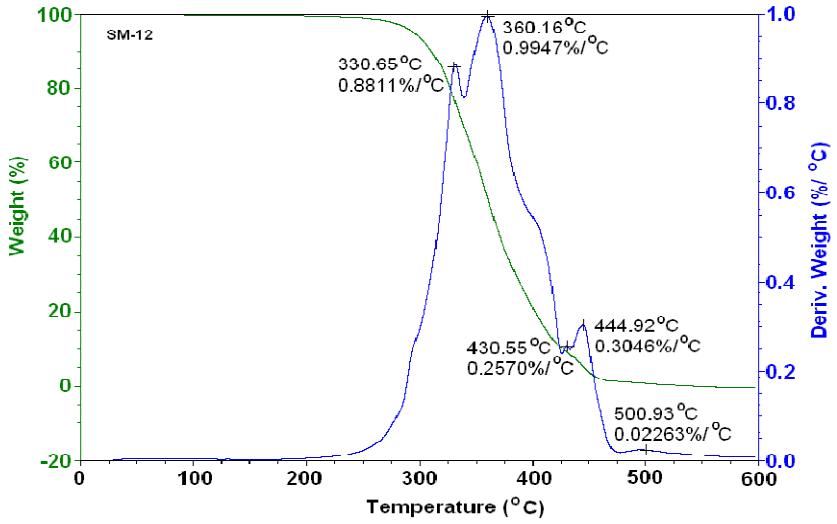

Fig. 3 Thermogravimetric and derivative curves of SM-12 (Neat PU of CO+HMDI)

The thermal stability of SM-12 and SM-15 were investigated by thermogravimetric analyzer (TGA). The degradation behaviour of the composites . The first degradation temperatures (T1), i.e. the temperatures at 5% weight loss of the nanocomposite (SM-15), with the exception of the control material was in the same neighbourhood of pure PU (SM-12) . The first degradation is mostly dominated by the degradation of organic modifier present in the clay. The derivative of the weight loss curves gave distinct degradation temperature peak (T2) , where the effect of clay particles is clearly seen. The T2 values of the nanocomposite are higher than those of pristine PU. This result indicates that clay–polymer reactions had almost no effect on thermal degradation behaviour. In the case of all the polyurethanes, a small % weight loss observed in the temperature range 100ºC - 200ºC is apparently associated with adsorbed water. At higher temperatures (300° C and 400° C), the weight loss observed in polyurethanes are 35%, 85% (SM-12) and 31%, 80% (SM-15) respectively at the same temperature thereby proving the higher thermal stability of the rigid polyurethanes.

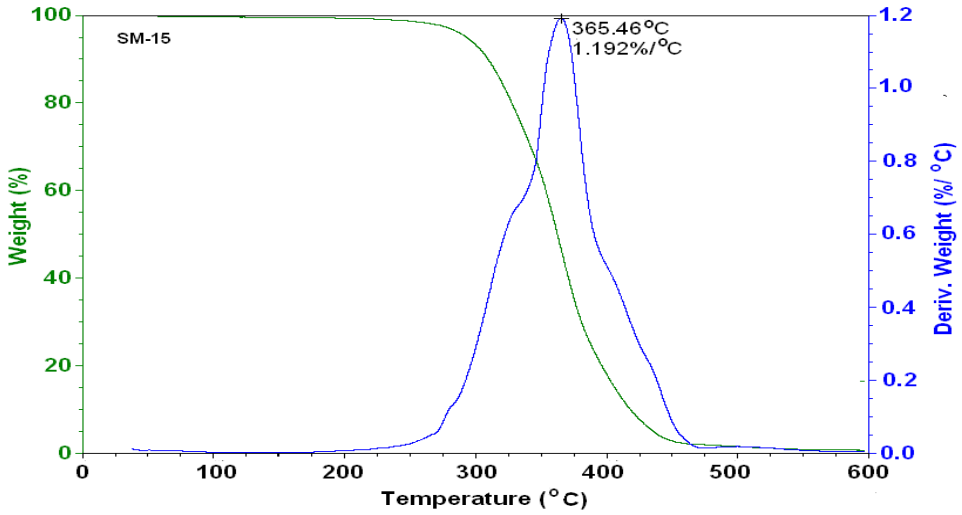

Fig. 4 Thermogravimetric and derivative curves of SM-15 (PU of CO + HMDI +2.5 wt % C30B)

1.5. XRD analysis

As a result, the XRD result indicates that the organoclay is highly exfoliated. XRD is generally employed to characterize the interlayer spacing in clay particles, which is correlated with their extent of intercalation. As the polymer chains are intercalated, the gallery height increases, resulting in the shift of characteristic, reflection to lower angles. If complete exfoliation takes place, no peak would be seen in the XRD pattern. The XRD of SM-15, where it can be seen that the diffraction peak for SM-15 appears at 20.3 A^o, when compared to 18.48 A^o for pristine C30B, suggesting the formation of intercalated tactoids .

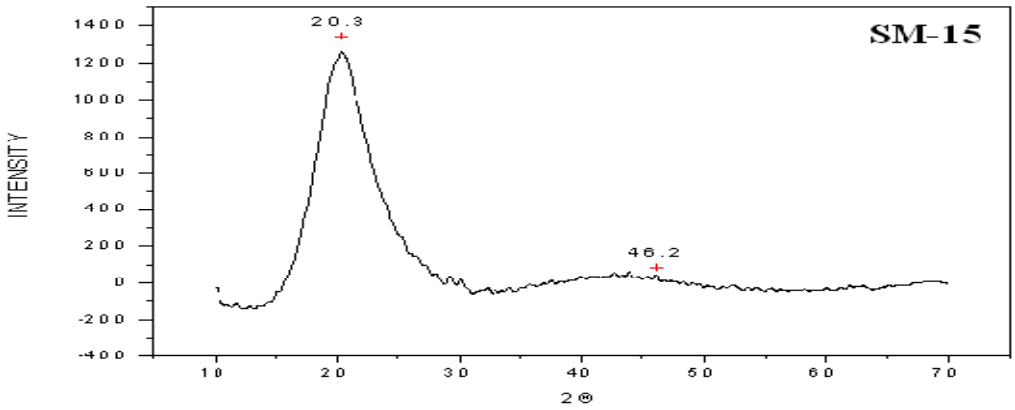

Fig. 5 X-ray diffraction analysis of PUNanocomposites of HMDI (with 0% and 2.5 % C30B in SM-12 and SM-15)

1.6. Tensile properties

Typical stress–strain diagrams of polyurethane and polyurethane composites of three varying amounts of clay . The modulus and tensile strength increased for all three clay loadings in composites of PU + HMDI. In the nanocomposite containing 5 wt% clay, the modulus and tensile strength increased by 110 and 170%, respectively, over pristine PU. Such improvement can be attributed to clay–polymer tethering as well as hydrogen bonding between clay particles and the polymer. Hydrogen bonding had much impact on the tensile strength. As already seen in , the values of NCO/OH ratios for the control material are similar to that of neat composites of the diisocyanates, although the value of tensile strength of PUNC of HMDI reported (4 MPa) is much smaller than that of the composite of TDI (12.8 MPa) with 5 wt% clay content. This indicates that hydrogen bonding did not contribute significantly to the tensile strength of the clay composites. The values of tensile modulus, on the other hand, were dominated by the clay particles. The strain at break did not improve as much in the presence of clay particles. This can be attributed to restrictions on the mobility of polymer chains during stretching by the tethering clay particles

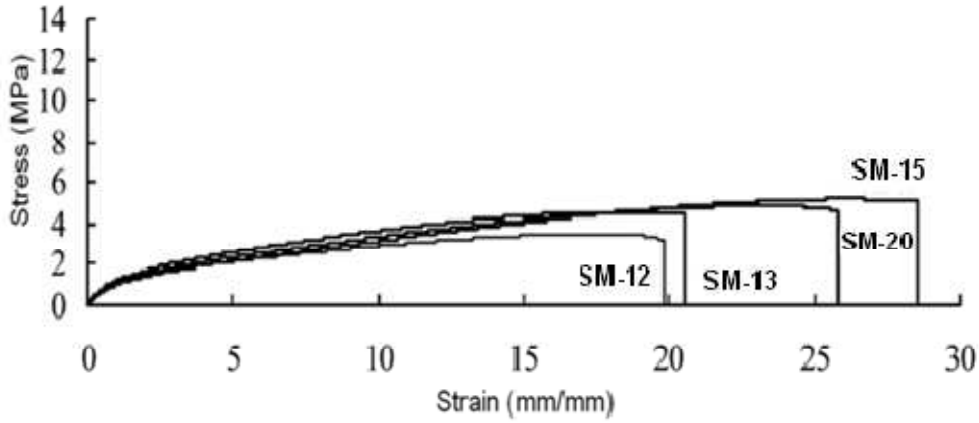

Fig. 6 Stress–strain diagrams of PU nanocomposites of HMDI with varying % of C30B

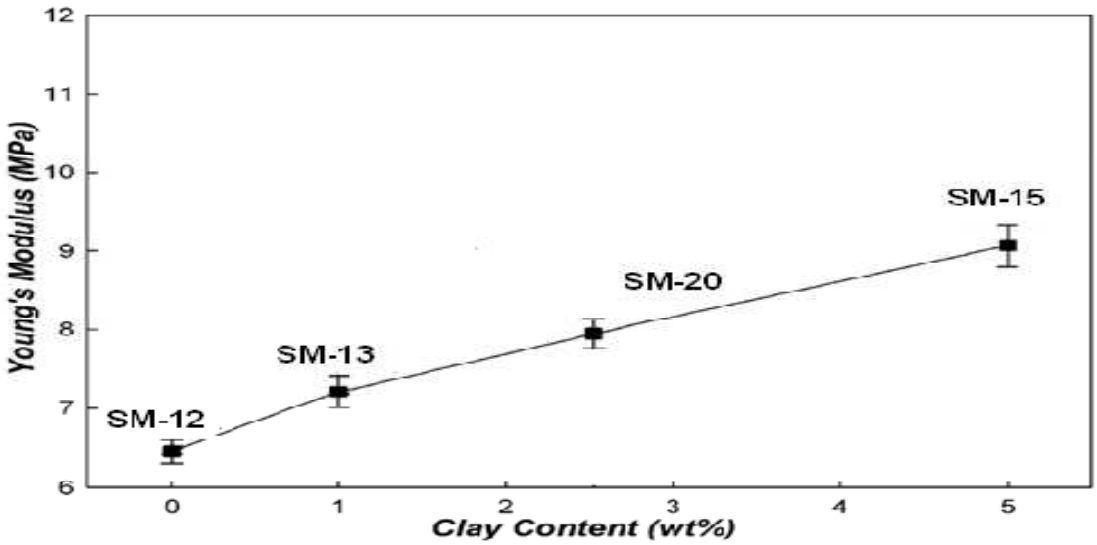

Fig. 7 Effect of clay loading on Young's modulus in PUnanocomposites of HMDIC30B

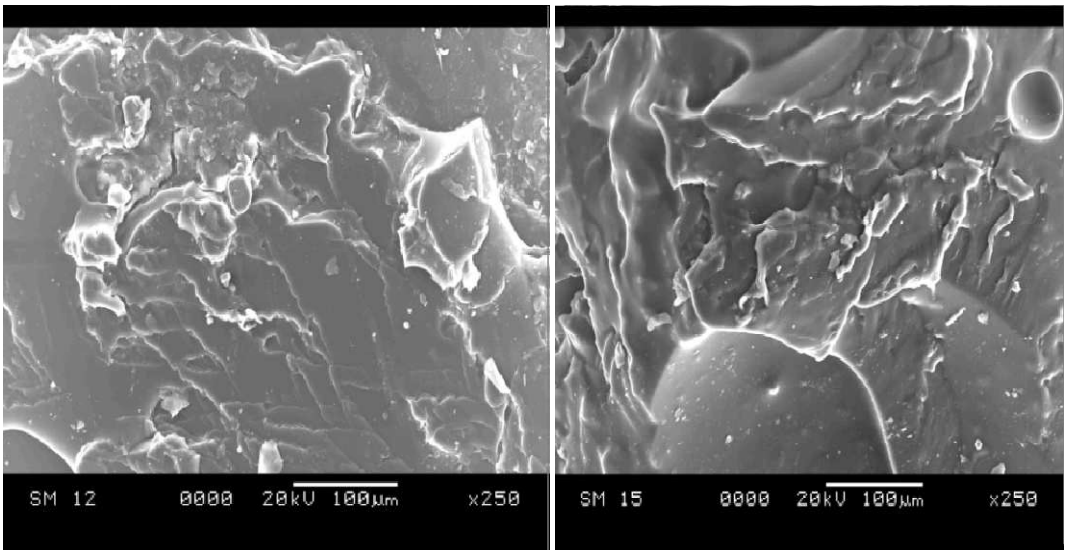

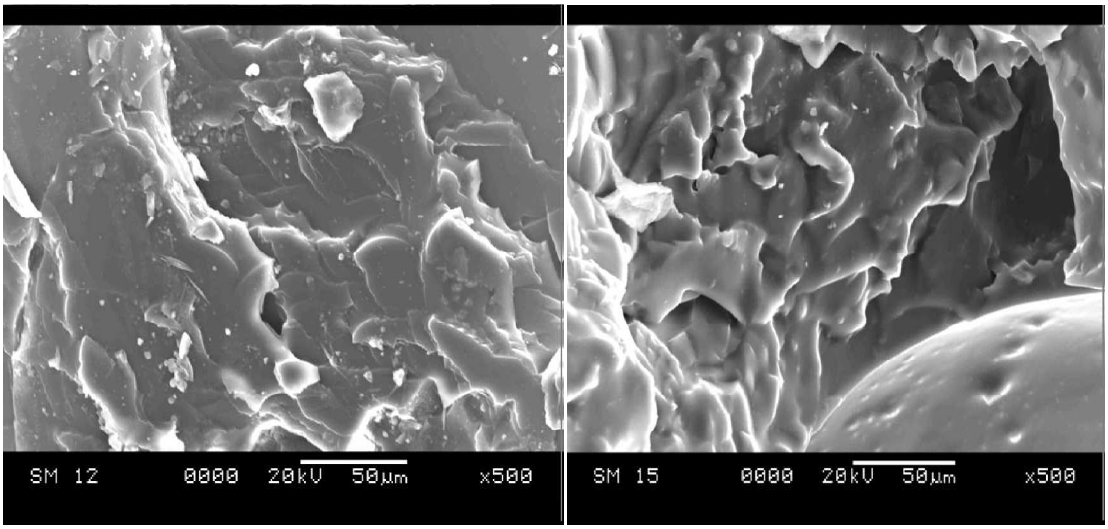

Fig. 8 Scanning Electron Micrograph (SEM) of PU Nanocomposites of HMDI

1.7. SEM studies

In the SEM, the gray coloured regions indicate the bulk of the polymer matrix and the brighter spots indicate the distribution of clay particles. However, the phenomenon of exfoliation, intercalation and aggregation is difficult to study from SEM conclusively, which can be easily reflected from TEM photomicrographs and XRD studies. The cross-sectional area of the SM-12 (neat COPU of HMDI) was smooth and dense, with no evidence of pores or channels. On the other hand, the SM-15(PU-NC with 2.5% C30B) surface was completely rough due to the homogeneous distribution of the clay aggregates in the polymer surface (**Fig. 8**). This could be attributed to the chemical interactions between the polar clay surface and polar urethane bonds present in the segments of the polyurethane.

Since no large clay aggregates could be observed on the fractured surface of the samples, it can be suggested that the procedure can be utilised for synthesis of polyurethane nanocomposites.

CONCLUSION

This study shows that covalently linked PU/n-HMDI composite and the nanofibres of this composite were successfully collected by the electrospinning process. The morphological appearance of the composite was smooth and uniform in size, with no visible n-HMDI particles on the surface. These high-surface-area nanofibres could potentially be used in biomedical and dental applications because of their bioactivity and because their mechanical properties can be adjusted to suit. The synthesis of ordered polyurethane from , hexamethylene diisocyanate (HMDI) . Hydrophobic nanoparticles and nanocomposite of 1,4-hexamethylene diisocyanate (HMDI)-modified PU nanoparticles (PU-NPs) have been synthesized at ambient temperatures. The platelet-like nanocrystals become pseudospherical after modification with HMDI and the size increases or decreases depending on diisocyanate concentration compared to the ungrafted particles as revealed by scanning electron microscopy (SEM) results. The obtained nanocrystals were characterized by means of the FT-IR and X-ray diffraction (XRD) techniques. When compared with the hydrophobic performance of the unmodified starch nanocrystals, that of crosslinked starch nanocrystals significantly increased. X-ray diffraction reveals that the crystalline structure of modified starch nanocrystals was preserved. The resulting hydrophobic starch nanoparticles are versatile precursors to the development of nanocomposites. The polyether-polyurethane crosslinked with UP-NPs nanocomposite exhibited thermo-responsive electrical conductivity.

REFFERENCES

[1] Williams DF. Biodegradation of surgical polymers. J Mater Sci **1982**;17:1233–46.
[2] Rehman IU. Biodegradable polyurethane: biodegradable low adherence film for the prevention of adhesions after surgery. J Biomater Appl **1996**;11:182–257.
[3] Bouchemal K, Brianc_on S, Perrier E, Fessi H, Bonnet I, Zydowicz N. Synthesis and characterization of polyurethane and poly(ether urethane) nanocapsules using a new technique of interfacial polycondensation combined to spontaneous emulsification. Int J Pharm **2004**;9:89–100.

[4] Kuan HC, Chuang WP, Ma CCM, Chiang CL, Wu HL. Synthesis and characterization of a clay/waterborne polyurethane nanocomposite. J Mater Sci **2005**;40:179–85.
[5] Liu Q, de Wijn RJ, van Blitterswijk AC. Nano-apatite/polymer composites: mechanical and physiochemical characteristics. Biomaterials **1997**;18:1263–70.
[6] [6] Tang RYW, Gonzalez JB, Roberts GD. Polyurethane elastomer as a possible resilient material for denture prostheses: a microbiological evaluation. J Dent Res **1975**;54:1039–45.
[7] Goldberg AJ, Craig RG, Filisko FE. Polyurethane elastomers as maxillofacial prosthetic materials. J Dent Res **1978**;57:563–9.
[8] Labella R, Braden M, Deb S. Novel hydroxyapatite-based dental composites. Biomaterials **1994**;15:1197–200.
[9] Ritter AV, Swift Jr EJ. Medium-viscosity polyether impression material: a case report. Comp Cont Ed Dent **2000**;21:993–6.
[10] Wakasa K, Yoshida Y, Ikeda A, Natsir N, Satou N, Shintani H, et al. Dental application of polyfunctional urethane comonomers to composite resin veneering materials. J Mater Sci: Mater Med **1997**;8:57–60.
[11] Whitworth JM, Makhani SH, McCabe JF. Cure behaviour of visible light-activated pattern materials. Int Endo J **1999**;32:191–6.
[12] M. N. Sreejayan-Rao, "Nitric Oxide Scanvenging by Curcuminoids," *Journal of Pharmacy and Pharmacology*, Vol. 49, 1997, pp. 105-107.
[13] H. P. Ammon and M. A. Wahl, "Pharmacology of Cur-cuma Longa," *Planta Medica*, Vol. 57**,** 1991, pp. 1-7.
[14] Brouet and H. Ohshima, "Curcumin, An Anti-Tumour Promoter and Antiimflammatory Agent, Inhibits Induction of Nitric Oxide Synthase in Activated Macro-phages," *Biochemical and Biophysical Research Communications*, Vol. 206, 1995, pp. 40-533.
[15] P.L Nayak and T . Pattnaik " Polymer from renewable resources II : Castor oil Based interpenetrating polymer networks : swelling behavior, scanning electron microscopy and x – ray diffraction" Macromolecular Reports, **1994**,3 : 447
[16] P.L Nayak, S. Lenka and T . Pattnaik " Polymer from renewable resources III:Thermal analysis of the internepetrating polymer networks derived from Castor oil –polyurethane- polyacrylate : swelling behavior, scanning electron microscopy and x – ray diffraction"Thermochemichimica Acta, **1994**,240 : 235-246
[17] P.L Nayak, and D.parida " Polymer from renewable resources IV: Castor oil Based interpenetrating polymer networks derived from isophorone diisocyanate poly (acrylamide) and poly (methacrylamide)"J. Applied Science, **1994**,46 : 1250
[18] P.L Nayak , S.K Swain and S.Sahoo" Polymer from renewable resources V : Synthesis and characterization of thermosetting resins derived from cashewnut-shell liquid (CNSL) furfural-substituted aromatic compounds," J. Applied Science,, **1994**,5 : 413
[19] P.L Nayak , S.K Swain, S. Lenka and S.Sahoo" Polymer from renewable resources VI : Synthesis and characterization of thermosetting resins derived from cashewnut-shell liquid (CNSL) formaldehyde-substituted aromatic compounds," J. Applied Science,**1995**,1 : 233